FINAL REPORT:

Topic:

A Novel Augmentor that Does Not Use Flame Holders to Stabilize the Combustion Process

Investigation of Auto-Ignition of Jet-A Liquid Fuel Injected Across the Flow of Hot Vitiated Air

Dr. Ben T. Zinn, Dr. Eugene Lubarsky, Dr. Yedidia Neumeier, and Aimee Williams
School of Aerospace Engineering
Georgia Institute of Technology
Atlanta, Georgia 30332-0150
Email: ben.zinn@ae.gatech.edu
Tel: 404-894-3033

Contract monitor:
Mr. Larry Goss
Innovative Scientific Solutions Inc (ISSI)
2766 Indian Ripple Rd
Dayton, OH, 45440

June 29, 2012

Abstract

This report describes the process of determining auto-ignition delay of the liquid Jet-A aviation fuel injected in a cross flow of vitiated air. Auto-ignition delays were measured by processing of the time-averaged chemiluminescence images for a range of temperatures from 898-1028K, vitiated oxygen percentages from 9.3% to 12.2%, velocities from 80 – 140 m/s and global Jet-A to, vitiated-air mixture equivalence ratios from φ=0.3 to φ=1.5. It was found that ignition delay increases exponentially from one to ten milliseconds with inverse temperature variation and are more scattered at lower temperatures. The data obtained in this study reveals delay times much shorter than those measured in most of other studies, but with same character of dependence upon the temperature of the flow.

Introduction

Traditional thrust augmentors of turbo-jet engines use a system of bluff body flame holders in combination with upstream fuel bars to form a combustible mixture and recirculation zones in order to hold a flame. While these devices are a useful method for increasing thrust, they cause a large pressure drop, require additional engine length and weight, and often lead to unstable combustion.This study investigates approaches to a novel augmentor without bluff body flame holders in which flame stabilization is based on auto-ignition of liquid fuel injected into the crossing flow of the hot vitiated air.

Auto-ignition is the process by which liquid fuel injected into a hot flow creates spray, evaporates, mixes, and ignites without an external ignition source. This is the process that scramjets, pulsed detonation engines, and diesel engines employ. The time from injection to ignition, known as ignition delay, is the key parameter, which determines the engine design. With liquid, non-premixed fuels, the time between fuel injection and ignition can consist of a physical delay of spray formation, evaporation, mixing and a chemical delay during which the chemical reaction between the fuel and oxidizer raises the temperature and the reaction rate until ignition occurs [1,2].

Several studies have determined the auto-ignition delay of kerosene-air mixtures in continuous flow combustors in the past 70 years. In 1952, Mullins published *Studies on the Spontaneous Ignition of Fuels Injected into a Hot Air Stream, Part I-Part VIII*[2], which cataloged many auto-ignition tests performed in a auto-ignition test rig developed by the National Gas Turbine Establishment from 1945-1947. The test section of this rig is presented in Figure 1-a as a 3° diffuser with fused silica observation windows. A T-scheme combustion chamber upstream of the test section provided incoming air temperatures between 400°C and 1100°C and velocities 31-270 m/s. The standard ignition delay measurement technique used was to inject fuel into the air flow and gradually raise temperature until the fuel ignited near the open end of the diffuser. The system was undisturbed for 5-10 minutes, allowing for conditions of thermal equilibrium to be reached and then the distance of the flame front from the entry was measured using a scale affixed to the rig. An example of results from this study is shown in Error! Reference source not found.. The author found that smaller droplet size and higher preheat temperature of the fuel

decreased the ignition delay while air-fuel ratio and velocity had no significant influence. Ignition delay was found to have an exponential dependence on temperature, which is shown as a linear fit in a log-linear *delay vs. T* scale.

a) b)

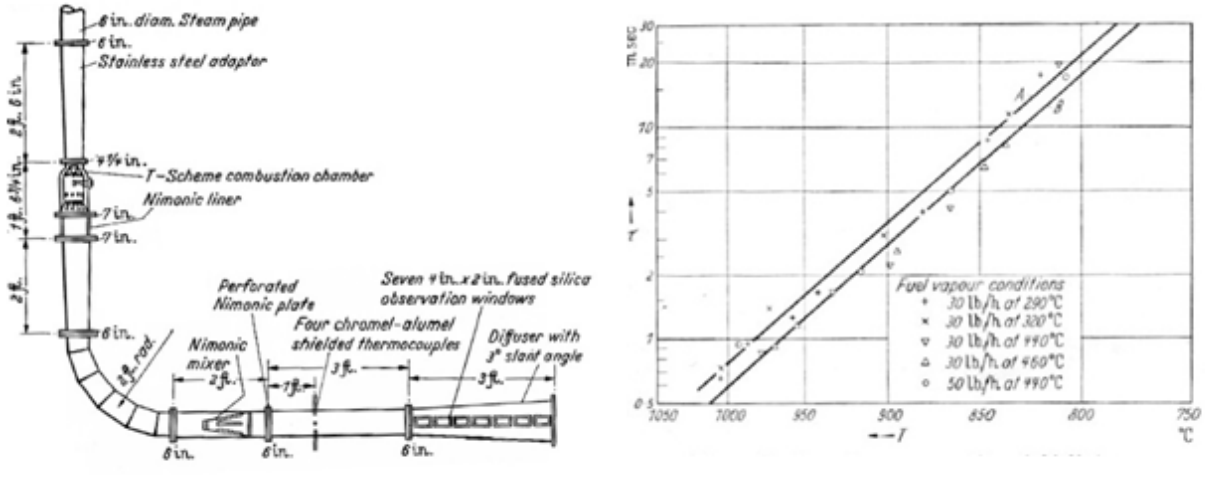

Figure 1. A schematic of experimental facility catalogued by Mullins's (a) and an example of test results (b)

Marek et al. [3], in 1977, determined auto-ignition delay times for liquid Jet-A fuel in a premixing, pre-vaporizing tube at high combustor inlet pressures and temperatures of 0.56 MPa to 2.5 MPa and 550 to 700K and lean equivalence ratios of φ=0.3 to φ=0.7. A schematic of the test facility is shown in Figure 2. A 25% open area un-cooled perforated plate was used as a flame-holder. The procedure was to set an airflow rate, inlet temperature and pressure and then begin fuel flow at low equivalence ratio and slowly increase to φ=0.7 to determine if auto-ignition would occur. If not, the fuel was turned off, and the pressure was increased for another test. Marek et al. determined ignition delay as the distance between the injector and flame-holder divided by the flow velocity in the premixing tube. Their data was considerably scattered, as can be seen in Figure 3, but in general, ignition delay time was found to be proportional to the inverse of pressure.

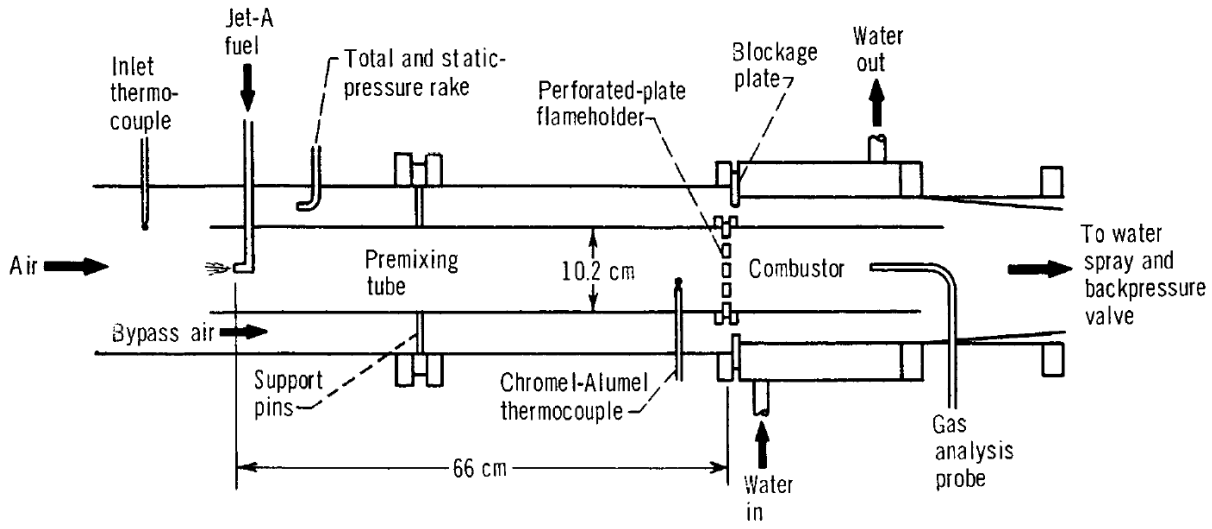

Figure 2. Schematic of test facility for Marek's auto-ignition study

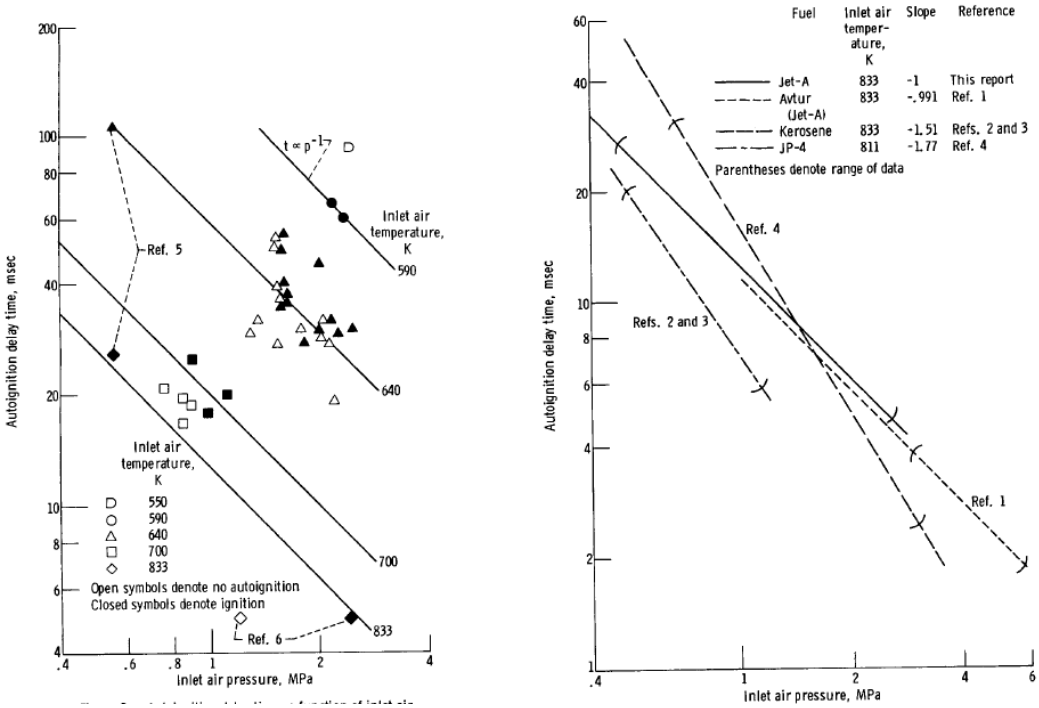

Figure 3. Auto-ignition delay time results from Marek et al. as a function of pressure

In 1980, Spadaccini and TeVelde [4] measured the auto-ignition delay time of Jet-A, JP-4, No. 2 diesel, cetane, and ERBS fuels. Their experimental setup shown in Figure 4 included an electric, air heater, an inlet plenum and flow straightener, a co-stream, multiple source injector, shown in Figure 5, a cylindrical mixer/vaporizer section that could be varied in length from 2.5cm to 150 cm, an expanding section with water quench to prevent flashback, a variable area orifice and a

scavenger afterburner. Their operating procedure was to establish a predetermined flow condition and increase temperature until auto-ignition occurred. Auto-ignition was simultaneously indicated by a thermocouple in the expander section, photo-detectors at several locations, a differential pressure transducer measuring the pressure drop across the mixer/vaporizer section and absolute pressure transducers in the mixer/vaporizer section. An example of the auto-ignition delay data from this study is shown in the Figure 6. Spadaccini and TeVelde found shorter auto-ignition times than previous studies, including the previously mentioned Mullins study, at temperatures above 775K, which they attributed to their use of a multiple source injector. They found no significant difference in fuel heating to 400K. They explained this effect by not significant influence of fuel heating upon the spray formation. Due to their calculations droplet diameters varied from 30μm to 26μm (foe non-heated to heated fuel respectively), therefore vaporization distance was not changed drastically. As expected, ignition delay time decreased as temperature, pressure, and fuel/air ratio increased. Spadaccini and TeVelde also found that the degree of mixture non-uniformity, indicated by the fuel concentration profile, has an important effect on ignition delay, as well as did airstream cooling due to fuel heating, vaporization, and convective heat loss. This observation is significant to note when considering the effect of global fuel to air ratio on ignition delay.

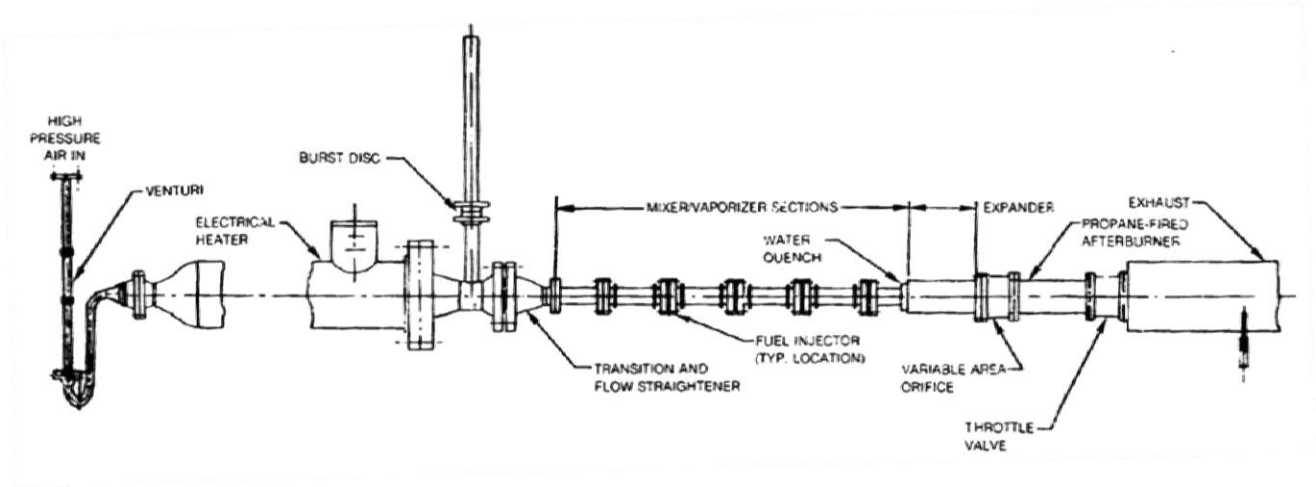

Figure 4. Spadaccini and TeVelde test rig schematic

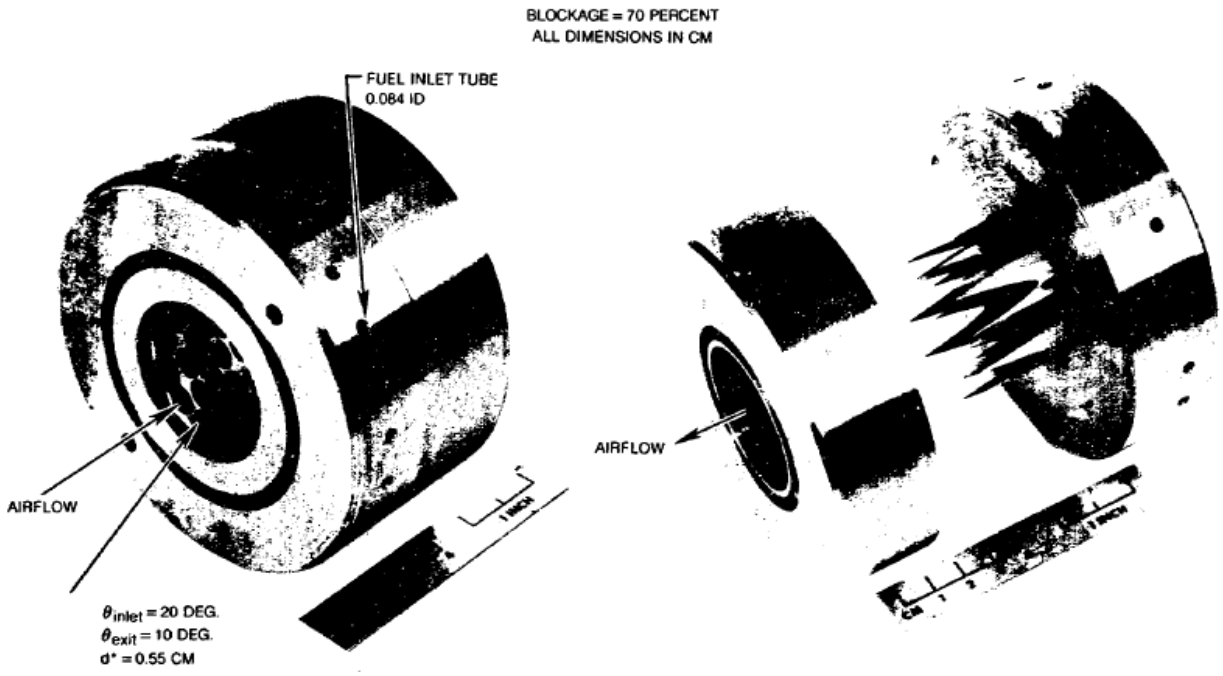

Figure 5. Multiple source fuel injector used in Spadaccini and TeVelde test facility

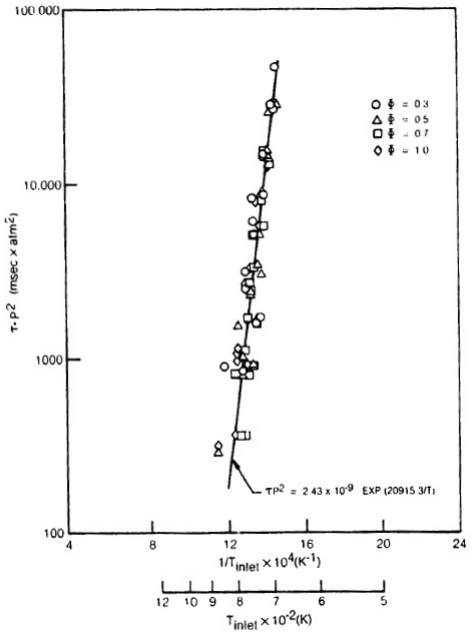

Figure 6. Example of test results from Spadacinni and TeVelde study

Tacina, in 1983 [5] measured auto-ignition delay times of No. 2 diesel fuel in a 12 cm inner diameter insulated flow reactor. Air supplied to the reactor was preheated using a hydrogen burner. A hydrogen enriched afterburner was located downstream of the test section to burn the remaining fuel. Both a single simplex pressure atomizer and multiple source fuel injector (see

Figure 7) were used. An example of the experimental data is shown in Figure 8. Tacina found that ignition delay depends upon the fuel injector type and was also a function of equivalence ratio for the multiple source injectors but not the for the simplex atomizer.

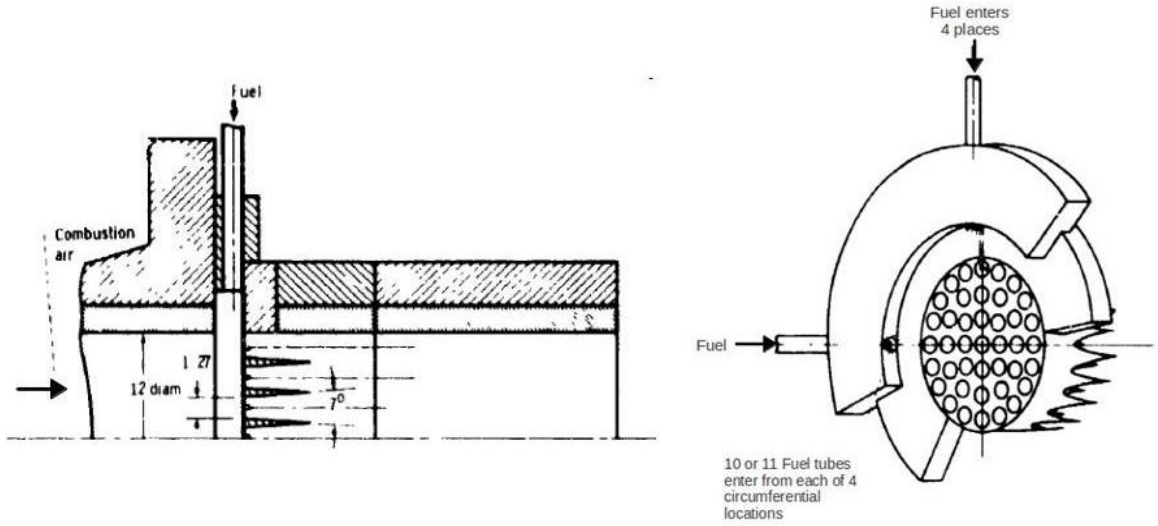

Figure 7. Schematic of a multiple source fuel injector used in auto-ignition experiments by Tacina

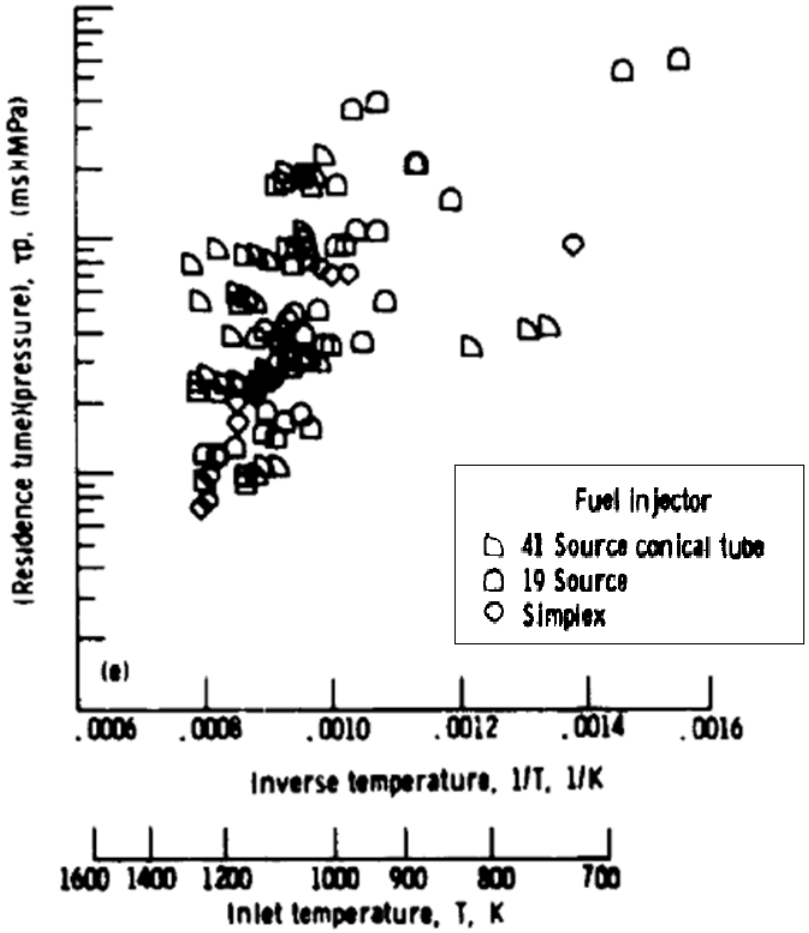

Figure 8. Tacina test data for simplex atomizing injector and multiple source injectors, plotted as the product of ignition delay and test section pressureversus temperature

Freeman and Lefebvre [6] measured spontaneous ignition delay times of gaseous and vaporized fuels in 1984. Their facility utilized air flow which was electrically preheated to a maximum temperature of 1150K at velocities from 10 to 40 m/s. Fuel was pumped from a reservoir through the electrical fuel vaporizer to the fuel injector that was designed to achieve rapid mixing of the fuel and air and attain uniform mixture. This was done by distributing 25 injection orifices over the entire cross-sectional area of the 12cm inner diameter insulated tubular duct. The fuel injector is shown in Figure 9. The test section was a constant diameter (I.D.=6.22cm), **??? cm** long of insulated stainless steel tube. Thermocouples were located at the fuel injection plane, 18cm downstream of the injection plane, halfway down the test section and at the end of the test section. The operating procedure was to set the flow conditions to predetermined values of velocity, temperature, and equivalence ratio and increase the temperature until ignition occurs downstream of the test section. The temperature was then increased again until the flame location moved upstream and was located near the exit of the test section. The delay time was determined as the length of the test section divided by the average velocity.

Author found that ignition delay was strongly dependent on the oxygen concentration in the tested range 16% to 51% of O_2. Ignition delay decreased as oxygen concentration increased. Dependence of the ignition delay upon temperature at different oxygen concentrations is shown on the Figure 10. At the same time Freeman and Lefebvre noted negligibly small dependence of the ignition delay upon the equivalence ratio in the range from φ=0.2 to φ=0.8.

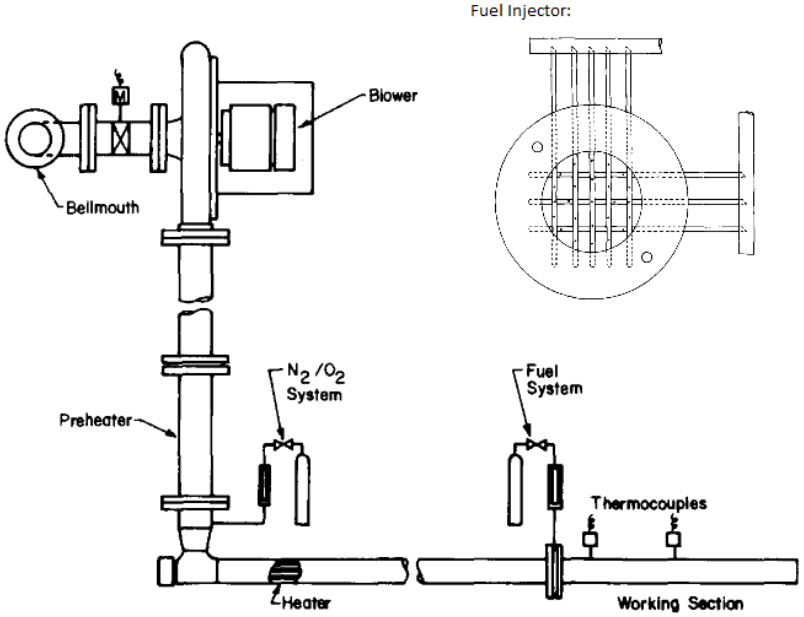

Figure 9. General schematic of the Freeman and Lefebvre test facility and schematic of the fuel injector designed for rapid mixing

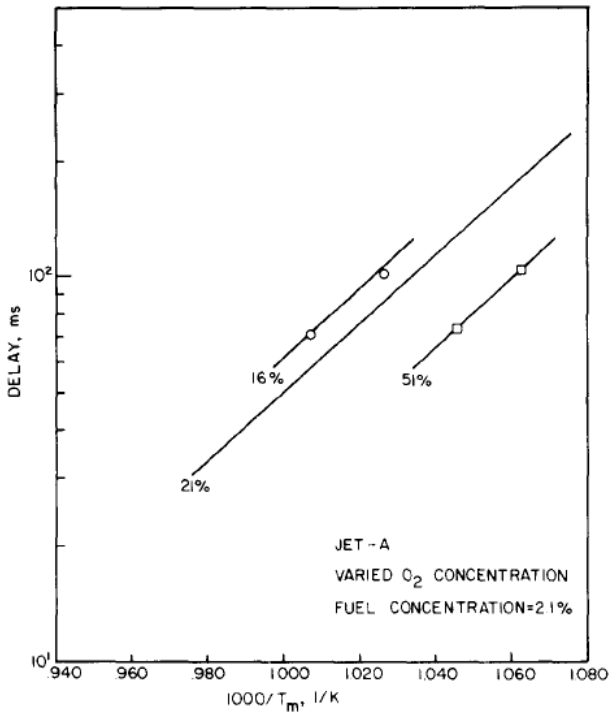

Figure 10. Dependence of ignition delay upon temperature of the flow at different oxygen concentrations obtained by Freeman & Lefebvre

More recently, Gokulakrishnan et al. [7-8] have completed experimental studies to validate a kinetic model of liquid fuel auto-ignition. Their test facility consisted of an atmospheric pressure reactor, fuel vaporizing system, fuel-to-air premixing section with swirler shown in Figure 11, and test section. The fuel vapor was passed through solenoid valves and time between the solenoid valve signal and the light emission to a photo diode recording the chemiluminescence emission was defined as the time delay. Ignition delay time was measured at temperatures from 900 to 1075K and at equivalence ratios of 0.5, 1.0, and 1.5. Data for ignition delay at an equivalence ratio of 1.0 is shown in Figure 12.

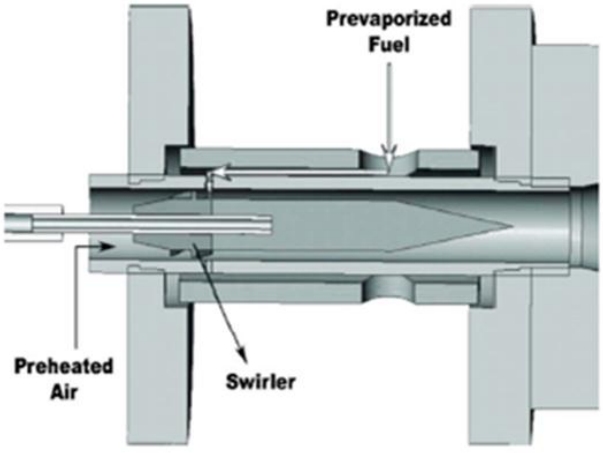

Figure 11. Premixing section used in the auto-ignition delay time validation experiments by Gokulakrishnan et al.

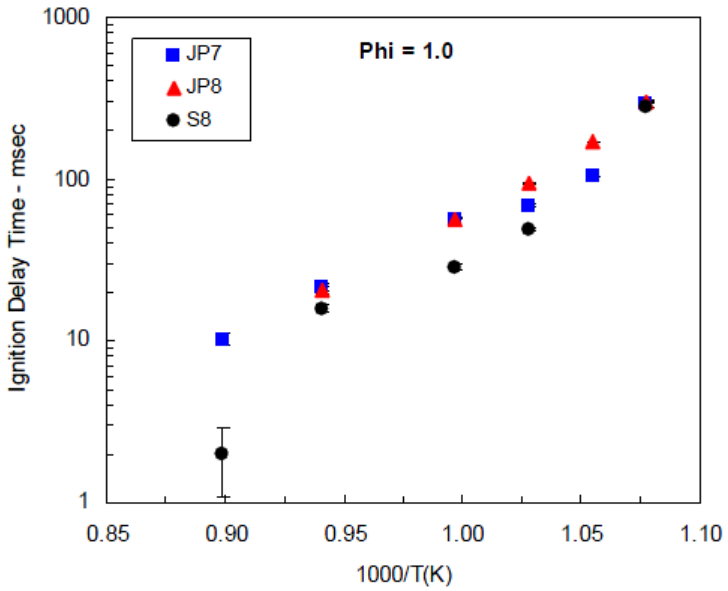

Figure 12. Dependence of ignition delay times upon temperature obtained by Gokulakrishnan et al.

Recent studies of the novel afterburner concept at Georgia Tech by Birmaher et. al. and Cutright et al. [9-11] observed auto-ignition of Jet-A liquid fuel injected upstream of the simulated turbine stage. These authors indicated that location at which fuel auto-ignites depends on the vitiated air velocity and temperature. An example of the data obtained in this study is shown in Figure 1313 in the form of CH* chemiluminescence and temperature distribution along the combustor. The two plots and images clearly show that both ignition location and the amount of fuel burned in the test section depend upon temperature, with the higher flow temperature case auto-igniting further upstream and burning more fuel in the simulated augmentor.

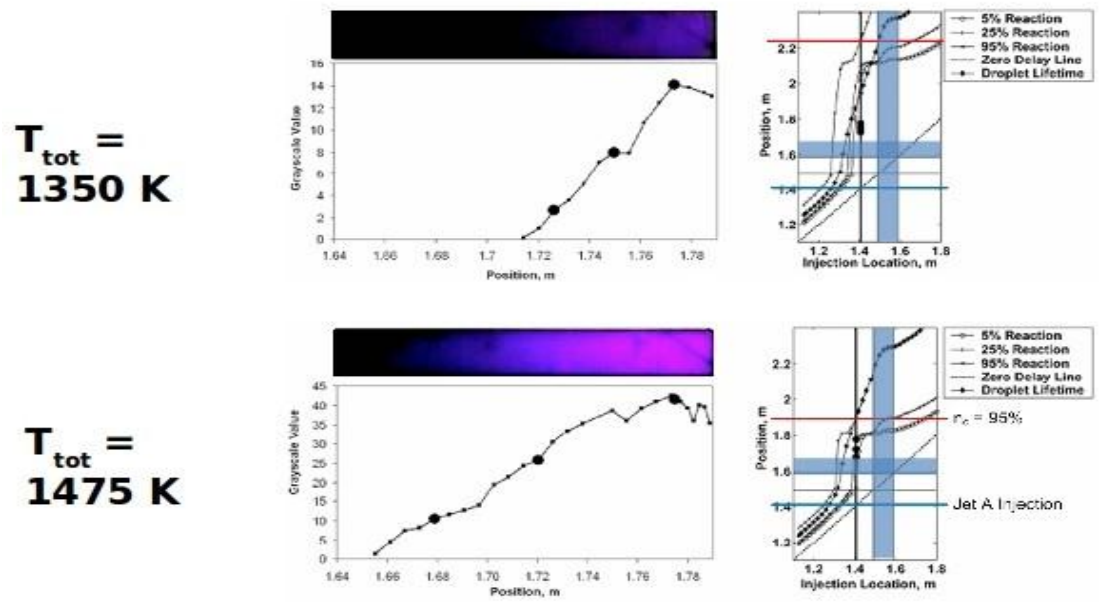

Figure 13. Measured and predicted dependence of Jet-A auto-ignition location upon the vitiated air temperature obtained in GaTech studies byBirmaher et al.

These extensive experimental studies can be summarized as follows:

1. Auto-ignition tests have been performed over incoming air temperature range of 550-1375K, reported air velocities up to 275 m/s, equivalence ratio ranges from 0.2 to 1.5 and pressures from 0.33 to 30 atm. Ignition delay times have been recorded for vitiated air and oxygen concentrations of normal air and 51% oxygen. Calculated droplet diameters for fuel injected by atomizers have ranged from 26 to 100μm. In some experiments fuel was pre-vaporized.

2. Ignition delay was found to have an exponential relationship with the inverse of temperature. It is usually shown on a log-linear scale versus the inverse of the temperature.

3. Time delay was found to be proportional to the inverse of pressure. Oxygen content has a large effect on ignition delay which decreased as oxygen concentration increased. Some effect of droplet diameters, fuel temperature, flow turbulence and flow uniformity was observed. Air velocity and test section length have no effect on ignition delay.

4. Experimental results obtained by different researchers are conflicting on whether equivalence ratio has an effect on auto-ignition delay. This discrepancy can be explained by significantly different test conditions.

5. In spite of the extensive auto-ignition studies that have been completed, the auto-ignition of liquid fuels at jet engine augmentor conditions – e.g. high velocity, high temperature, with disintegration of liquid fuel jets incross-flow of vitiated air, has not been investigated to a necessary extend. Recent GaTech studies at the flow conditions of interest observed the effect of

temperature and velocity of the flow upon the position of fuel auto-ignition but do not provide quantitative data set, which is necessary for developing a design tool.

Current study seeks to quantitatively characterize the effect of variation of position of fuel auto-ignition in the test section upon temperature, oxygen concentration, and velocity of the vitiated air flow and provide an improved understanding of Jet-A combustion at afterburner conditions without flame stabilization by the bluff body. A high temperature, high velocity, atmospheric flow reactor, free of flow disturbances such as bluff bodies, dump planes, and swirlers, was used to best simulate a novel augmentor conditions. Fuel jets were injected into the high velocity cross flow of vitiated air to attain disintegration of jets into small droplets in the shear break-up regime. This jet in cross flow (JICF) injection scheme additionally minimizes disturbances to the incoming flow that can create local recirculation zones and thus initiate auto-ignition.

Experimental Facility and Methodology

High Velocity Ignition Facility

Experimental facility used for this study was designed to simulate flow conditions in a jet engine thrust augmentor. A schematic of the high velocity ignition facility (HVIF) is shown on the Figure 1414. This facility consisted of a stagnation point reverse flow (SPRF) combustor – vitiator, dilution section, flow conditioning – measuring section, liquid fuel injection section and transparent test section.

SPRF combustor was used in this rig due to potentially high combustion efficiency and minimum disturbances it may apply to the flow. Cold air was supplied to the SPRF combustor at the base of the SPRF, and then passes along the outside of the combustor can for cooling combustor and pre-heating flow. Natural gas and now pre-heated air were injected radially inward in distributed jets. The mixture is then impeded by a cylindrical insert and forced down to the base of the combustor can where a stagnation point was formed. A spark igniter with hydrogen purge was located at the base of the vitiator. Cold, diluting air was introduced in the form of cross-flow jets just downstream of the vitiator to allow for control of the temperature and oxygen content.

Air was supplied to vitiator and dilution section from the 125 psig laboratory air tanks and then was regulated to 40 psig.Total air flow rate was measured using an orifice plate equipped with upstream static pressure and differential pressure sensors and controlled by a manual gate valve. Diluting air was withdrawn from the total air flow rate and controlled via a manual gate valve.

Natural gas was supplied to vitiator from the city line at 32 psig and was also metered using an orifice plate and pressure transducer system and was controlled by a manual needle valve.

Flow conditioning – measurement section was a 2 inches diam. (I.D.=2.08 inches), 12 inches long stainless steel pipe with entrance end connected to the flange through which dilution air jets were injected. The other end of this pipe was connected to the fuel injection flange. The pipe was externally cooled using a system of air jets supplied from the shop air supply line. This pipe contains a Bosch LSU42 O_2 sensor with Innovate Motorsports 3769 LC-1 Wideband Controller Lambda Cable and a ¼” Omega K-type un-grounded thermocouple. Measuring devices we installed approximately four inches upstream of the point of fuel injection with minimized intrusion into the flow.

The liquid fuel injection section of the rig provided smooth transition from the I.D.=2.08 inches of the conditioning – measuring section to the transparent test section I.D=1.77 inches. Overall cone angle was 11° (5.5° per side). Two fuel injection ports were located near this cone termination approximately ½ inch downstream from the cylindrical test section entrance.Details of the fuel injection section are shown on the Figure 14 (on the right) with photographs of the section and injectors in the upper right corner. Cone termination was designed with a shoulder and soft graphite gasket to provide a support for the quartz tube test section. Liquid Jet-A fuel was injected through two 0.018" jet-in-cross-flow injectors drilled through the spherical terminations of the 1/16 inch diam. stainless steel tubes which were recessed approximately 0.1" into a 1/8" diam. holes in the conical part of the fuel injection section.

It is worth to note that this smooth conical transition was chosen following initial testing with abrupt changes of the area, which revealed flame holding near the fuel injection flange.

The test section consists of a quartz silica transparent tube I.D.=1.77" and 32.25" long with the lower end set upon the shoulder of the injection section and the other end near the tube termination supported by a clamp attached to the structure of the rig.

Flow velocity in the test section was calculated from the total air and natural gas flow rates, taking into consideration the density change due to vitiation. The calculation of a global Jet-A, vitiated-air mixture equivalence ratio was based upon the air and natural gas flow rates and a new stoichiometry calculated from the oxygen content of the vitiated flow. Equations 1-4 outline the procedure for calculating global Jet-A, vitiated-air mixture equivalence ratio.

$$\phi_{vit} = \frac{\dot{m}_{NG}}{\dot{m}_{air}} * 17.12 \tag{1}$$

$$O_2\% = 0.0223\phi_{vit}^2 - 0.231\phi_{vit} + 0.2094 \tag{2}$$

$$\bar{S} = 0.\frac{2095}{O_2\%} * 14.2467 + 0.42281 \tag{3}$$

$$\phi_{JetA} = \frac{\dot{m}_{JetA}}{\dot{m}_{air}+\dot{m}_{NG}} * \bar{S} \tag{4}$$

It is worth to note that this test facility was designed to achieve high velocities of the flow up to V=250m/s and temperature up to 900ºC. In fact, maximum velocity of the hot flow achieved in the reported test series did not exceed V=140 m/s at T=758°C. It seems that this limitation was associated with the fact that cylindrical insert of the SPRF combustor had flared outward due to overheating (this defect was discovered during rig disassembling after the test series ended). As a result, pressure growth in the clearance between combustor wall and cylindrical insert choked the natural gas flow and thus limited the maximum temperature the flow was able to achieve at high air flow rates (e.g. at high velocities of the flow in the test section).

Liquid Jet-A fuel was supplied from a one gallon double ended Swagelok DOT-3A1800 stainless steel high pressure cylinder shown on the Figure 15. This cylinder was pressurized from the top end with 50 psig nitrogen. The bottom end of the cylinder was used for supply and refueling. When supplying, fuel flows through an <Arrow>, 25 micron, in-line filter before metering in an <Omega> type FTB9501 turbine flow meter connected to FLSC-AMP <Omega> preamplifier

and DP-F31-LIN<Omega>display with linear corrector and analog output to the computer. A needle valve was used to control Jet-A flow rate and a 3-way valve switched the system from Jet-A flow to a nitrogen purge, which prevented injectors from clogging during gaps in the injection sequence.

Test Procedure

In a typical experiment, flow conditions were set to a desired temperature, velocity, and oxygen content using the air and natural gas flow rate and dilution air controls. Once the flow reached a steady temperature, Jet-A was injected at the first desired flow rate (resulting in a Jet-A, vitiated-air equivalence ratio of $\phi = 0.5$). At this flow rate and all proceeding flow rates, if auto-ignition occurred, a set of images was recorded and afterward, Jet-A flow rate was increased (up to $\phi = 1.5$ for this study). If flashback occurred during recording, which occurred only at the lowest velocities tested, then additional image sets were taken until an entire set was free of flashback phenomena. Once image sets were obtained for all desired fuel flow rates, new flow conditions were set and process repeated.

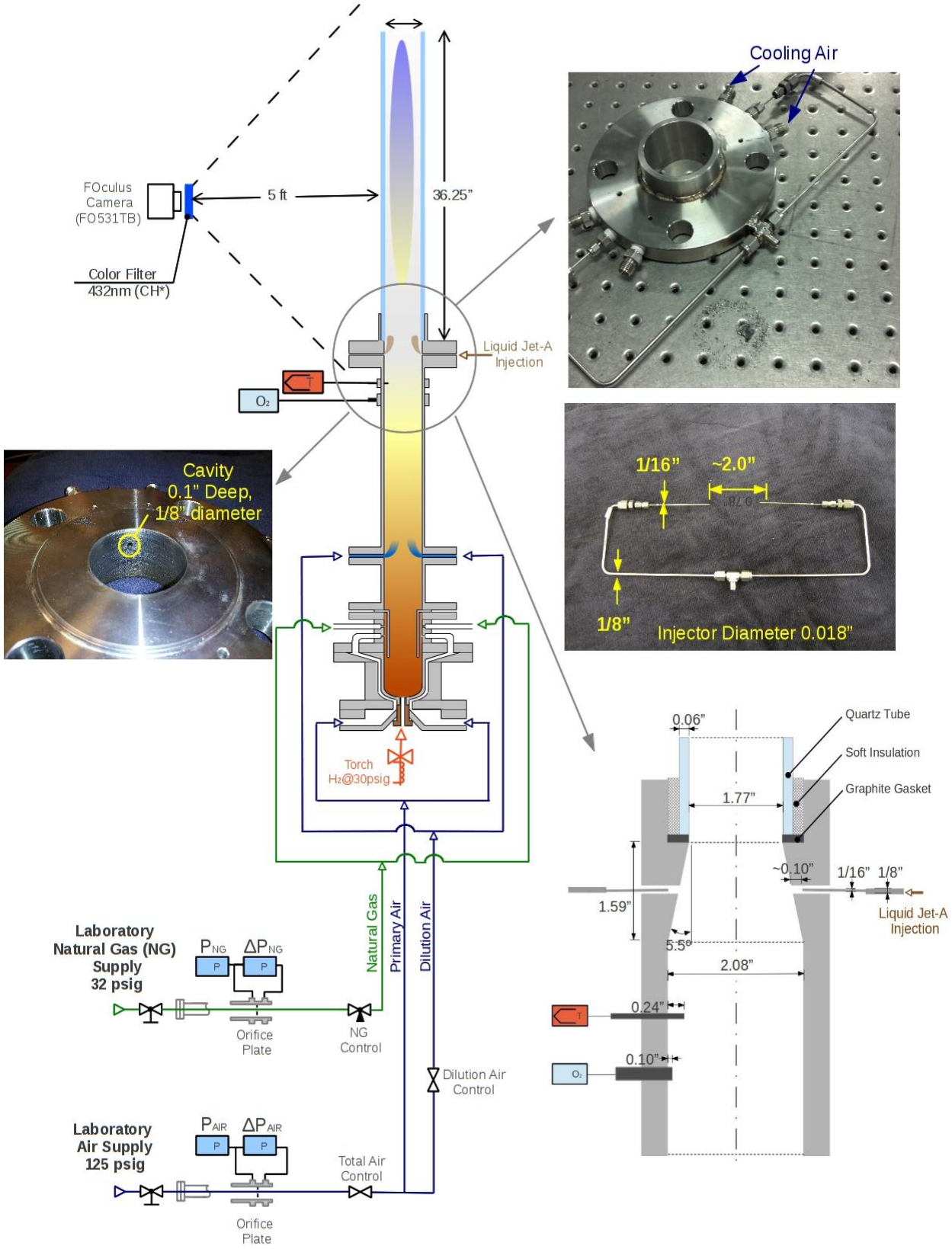

Figure 14. Schematic of the high velocity auto-ignition experimental facility

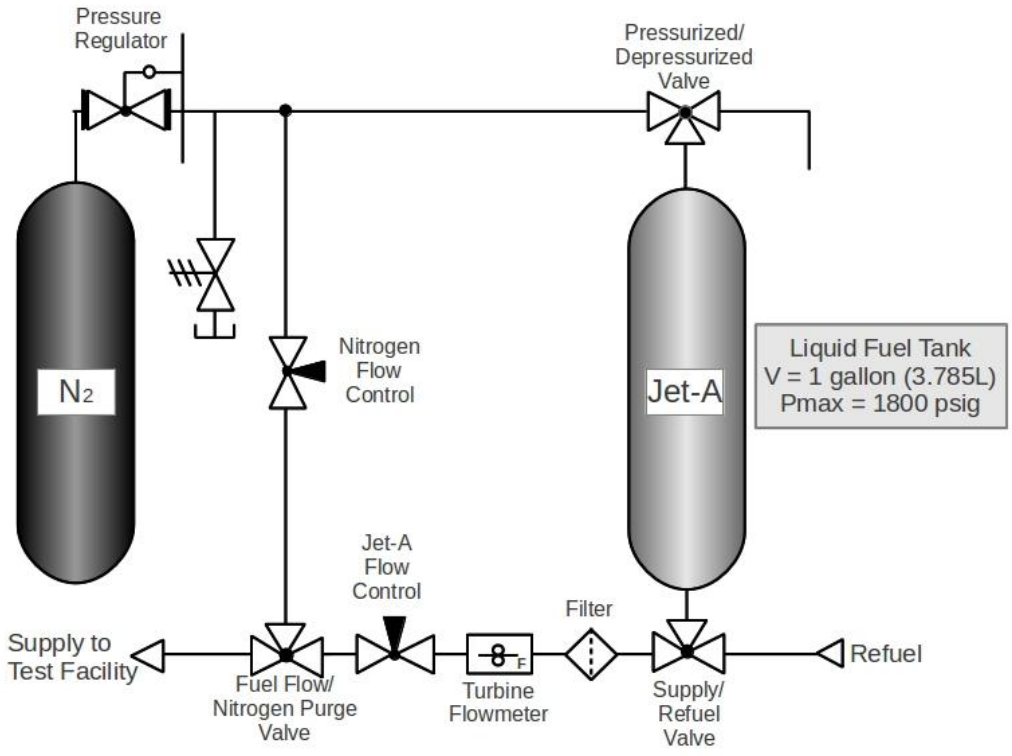

Figure 15. Schematic of liquid Jet-A delivery system

Data Acquisition and Processing

A FOculus CCD camera (FO531TB) with a 2.5mm lens and 432±10nm CH* filter were used to capture time averaged auto-ignition events. The camera was located approximately 5 feet radially from and aligned with the axial center of the test section and captured the entire length in a 1600x1200 pixel image**.** Table I shows the exposure time per frame and total frames per image set on each date of data collection. The camera placement is depicted on the Figure 14. A special marker indicating was illuminated using bright white light source to mark position of fuel injectors in each of the chemiluminescence images.

Table I. Exposure time and number of frames for each day of data collection

Date	Exposure Time (msec)	Number of Frames
20120606	621.0	6
20120611	1780.0	2
20120615	621.0	7

An example image set consisting of 6 frames taken at one flow condition is shown in Figure 16.

The yellow dashed line denotes the location of fuel injection. The CH* chemiluminescence, representing heat release, is visualized as the intensity of each pixel. It can be seen in these images that auto-ignition location is not constant in time, even for time average images at the same flow conditions. Note that the dark vertical band in the chemiluminescence images and the drop in intensity near 1300 pixels or 1100 mm are due to the clamp used to support the quartz tube.

Figure 16. Image set captured at flow conditions T = 983K, V = 142 m/s, O2% = 11.9, Φ_{JetA}= 0.78

Distribution of the reaction intensity along the test section was determined by integration pixels intensity in Y-direction at each pixel location along X-axis, with axes defined in the bottom right hand side of Figure 16. These distributions are shown plotted in Figure 17 at one flow condition. Location of fuel injection and the threshold applied to determine ignition location are superimposed on the plot. The threshold is 5% of the lowest maximum intensity of all images collected and the ignition distance is the location of fuel injection subtracted from ignition location determined by this threshold. The distances are transformed from units of pixels to meters using the conversion 1 pixel equals 0.84 mm in accordance to the resolution of the images. Finally, ignition delay time was determined as a distance from the injection point to the ignition location divided by average velocity in the test section as shown in the Equation 5.

$$t_{ign} = \frac{x_{ign}}{u_{avg}} \tag{5}$$

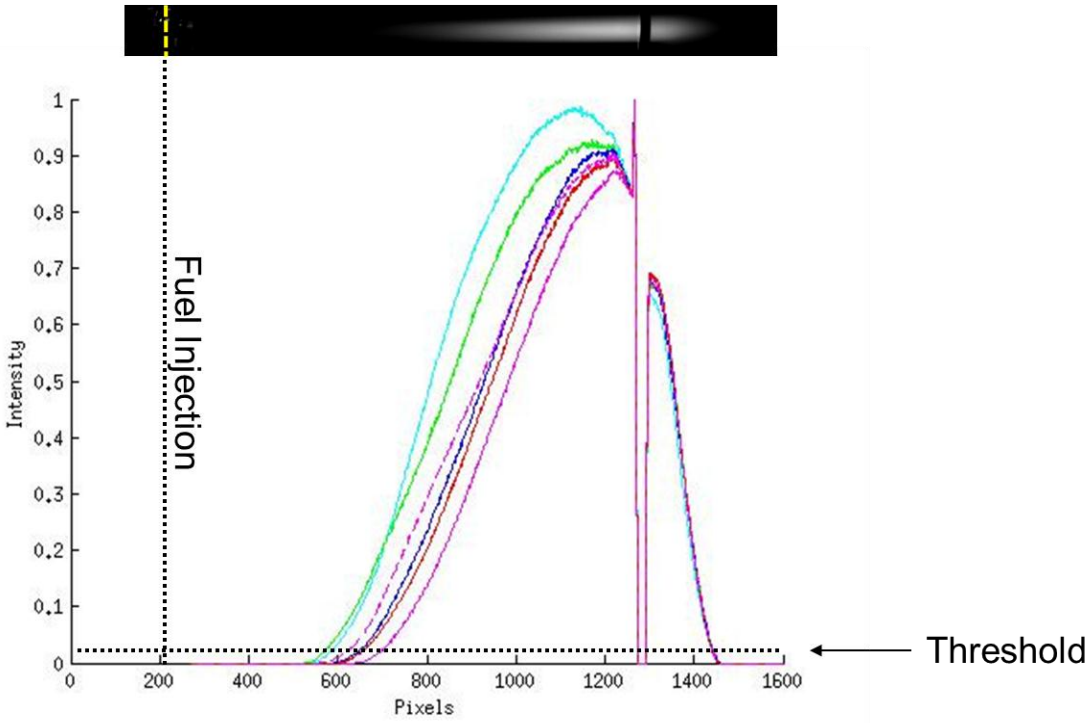

Figure 17. Reaction intensity variation plotted as function of distance (in pixels) for each image captured at T = 983K, V = 142 m/s, O2% = 11.9, Φ_{JetA}= 0.78 (from the set of images shown in Figure 16)

Results and Discussion

Auto-ignition delay times were measured for a range of temperatures from 898-1028K, O_2 = 9.3% to 12.2% of oxygen in the vitiated air flow, velocities from 80 – 140 m/s and global Jet-A, vitiated-air mixture equivalence ratios from φ=0.3 to φ=1.5, referred to as equivalence ratio from this point onward. The flow conditions and calculated auto-ignition delay times for all test conditions are tabulated in Appendix A. Each ignition delay time reported corresponds to the average of multiple ignition delay times at the same flow conditions, with the averaging process described in the previous section, Data Acquisition and Processing.

Examples of the chemiluminescence images obtained in this study and their corresponding integrated intensity plots are shown in Figure 18 through Figure 20. These Figures demonstrate variation of the location of the ignition point as a result of flow velocity, temperature, and equivalence ratio variation. These chemiluminescence images on these Figures are averaged over all frames in the image set at the specified flow conditions. The location of fuel injection is shown by a dashed yellow line on the images and corresponds to X=0 in the plots.

A comparison of the chemiluminescence images and resulting integrated intensity plots captured at different velocities of the flow, V=90.8 m/s and V=140.1 m/s, for a constant temperature of the flow, T=995K and equivalence ratio of approximately φ=0.43 are shown in Figure 18. The

images and plots show that as velocity is increased, the reaction moves downstream as well as auto-ignition location. Ignition delay time calculated as distance from the injection point to the point of auto-ignition divided by velocity of the flow was shown to be 1.8 ms and 2.6 ms for V=90.8 and V=140.1m/s respectively. In spite of the noticeable difference of 0.8ms this does not exceed repeatability error in the current experimental series and differences obtained by other researchers [2]. This result should be addressed in our future studies by widening the range of flow velocities (e. g. up to V=250m/s) at an increment which will allow the capture of possible trends of ignition delay upon flow velocity at constant temperature and equivalence ratio.

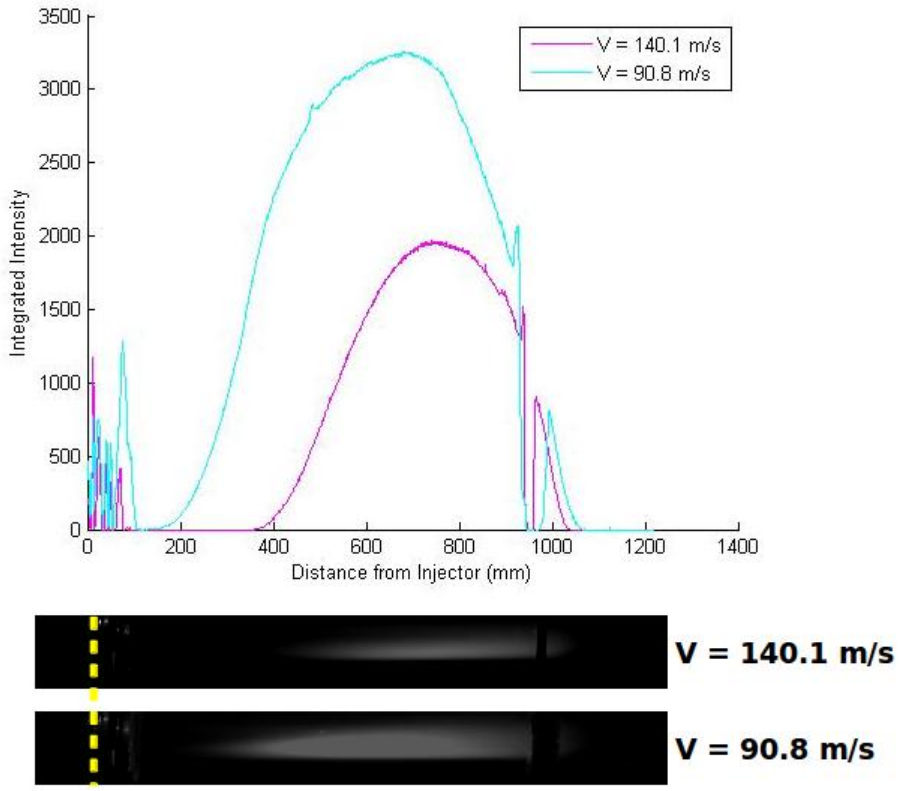

Figure 18. A comparison of auto-ignition images at different velocities, V = 140.1 m/s and 90.8 m/s at constant Phi=0.43 and T=995K

In Figure 19, chemiluminescence images and integrated intensity plots are shown for auto-ignition at different equivalence ratios of φ=0.411, φ=0.573, and φ=0.780 and constant velocity and temperature of V=141 m/s and T=983K. As expected, the greater equivalence ratios yield more luminous reactions. Plots of integrated intensities clearly show shortening of the distance from the point of injection to auto-ignition (e.g. shorter time delay as velocity was constant for all three measurements) at higher equivalence ratios at this flow conditions. They were found to be $t_{ign.}$=3.52ms, $t_{ign.}$=3.22ms and $t_{ign.}$=2.50 for φ=0.411, φ=0.573, and φ=0.780 respectively. On the contrary, at a higher temperature of the flow of T=1020K ignition delay was found to be independent of the equivalence ratio in the range of φ=0.34 to φ=0.80 and equal to $t_{ign.}$=1.6ms. Similar trend of ignition delay time upon the equivalence ratio was reported by other researchers

[4]. It should be noted however that some of the researchers found ignition delay time to be independent of the equivalence ratio. In the current study, we observed both trends in different incoming flow temperature ranges. This fact should be addressed in our future studies due to the significance of such dependence for design of a jet engine afterburner that operates in a wide range of equivalence ratios and incoming flow temperatures.

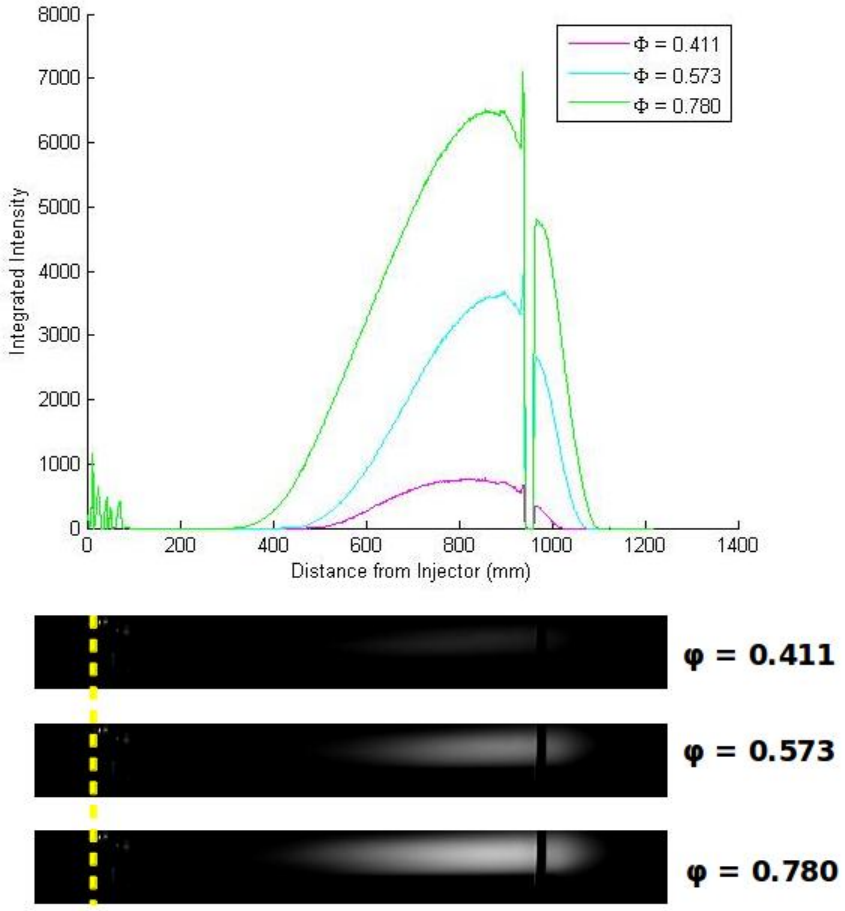

Figure 19. A comparison of auto-ignition at different equivalence ratios, ϕ = 0.411, 0.573, and 0.780 at constant V = 141 m/s and T = 983K

In Figure 20, the chemiluminescence and integrated intensity plots resulting from auto-ignition at the different vitiated air temperature of T=910K, T=916K and T=939K at the same velocity and equivalence ratio of V = 83m/s and ϕ = 1.45 are shown. It is clearly visualized, especially in the integrated intensity, that as temperature is increased, the reaction moved upstream and ignition delay time is decreased from t_{ign}= 6.63ms to t_{ign}=5.99ms and t_{ign}=5.82ms at the temperatures T=910K, T=916K and T=939K respectively. Definitely, this trend should be investigated in a wider temperature range in our future studies.

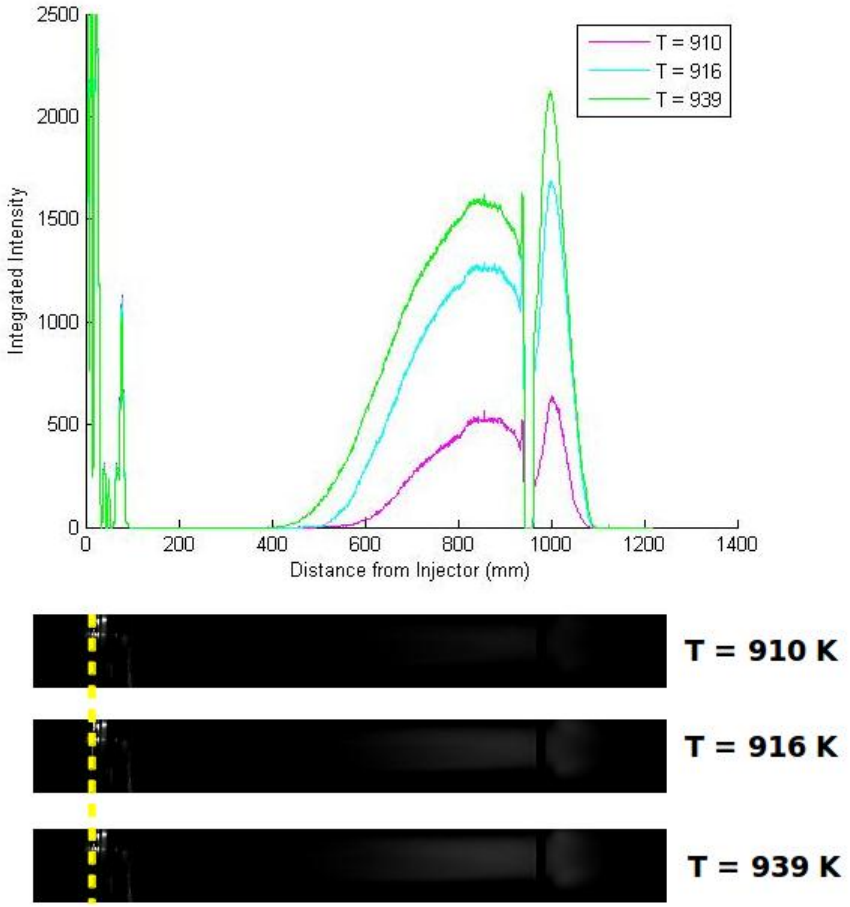

Figure 20. A comparison of auto-ignition at different temperatures, T = 910K, 916K, and 939K, and constant V = 83m/s and ϕ = 1.45

Figure 21 shows a comparison of auto-ignition delay times for all data collected. The shape and color of each data point describe the velocity and equivalence ratio at which the image set was recorded. In general, ignition delay time increases exponentially with the inverse of temperature. Spread of experimental data is much wider in the range of lower temperatures (T<950) then at higher temperatures. Such character of the ignition delay time dependence upon the temperature of the flow was observed by other researchers as well. Practically all researchers obtained exponential dependence of time delay over inverse temperature while only few of them admitted wide scattering of data especially at lower temperatures (see, for example Figure 8 in the Introduction). Possible reasons for data spread at lower temperatures in our study were as follows:

- Ignition time delay depends upon the equivalence ratio as it was shown in the Figure 19. The lower equivalence ratio conditions (blue and magenta colored data points on the Figure 21) have longer delay times than the higher equivalence ratio conditions.
- It was observed that at higher temperatures, the flame did not move in the test section as much as at lower temperatures. In fact difference in position of the point of auto-ignition on the images captured sequentially at the same flow conditions was at least four times

lower at high temperature comparing to the lower temperature data. This is clearly illustrated by the repeatability error bars superimposed on the Figure 21.

Experimental methodology of the current study may also play a role in data scattering. For example:

- Images captured at low equivalence ratio and low temperature conditions had very low intensity and this may contribute to the scattered data. A more sensitive camera in future tests may be useful to address this issue.
- In the high temperature range, T>950K (LHS of the abscissa on the Figure 21) ignition delay times are approaching the minimum measurement limit as ignition point moves upstream into the non-transparent section of the rig. Experimentation at higher velocities of the flow will shift point of auto-ignition further in the test section and thus extend our experimental capabilities to measure shorter time delays ($t_{ign.}$<1.5msec)

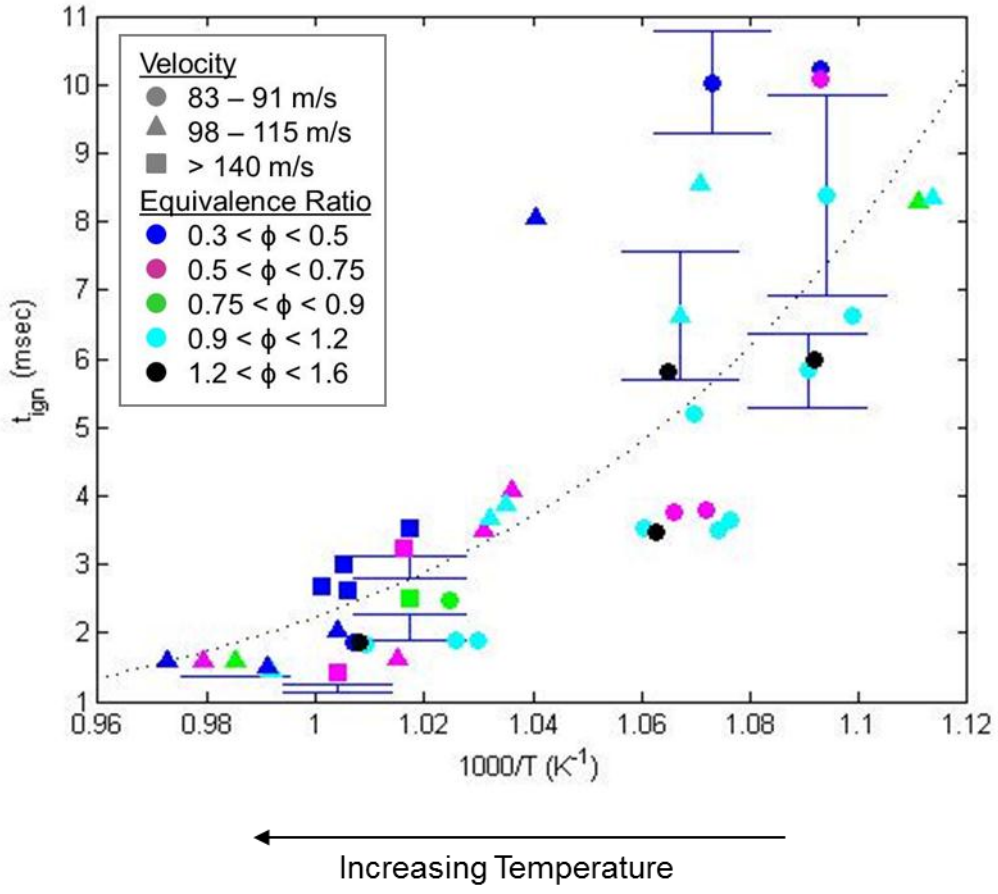

Figure 21. Summary of the test data obtained at all operating conditions tested.

In Figure 22, data collected in the current study is compared to data from some of the experiments mentioned previously in the Introduction. It is clearly seen that the obtained auto-ignition time delays are significantly shorter comparing to the most of other researchers. Especially, at the flow temperature of T=950K measured time delay was approximately 5msec

comparing to 100msec in (see Freeman and Lefebvre as well as Gokulakrishnan data on the Figure 22). Mullins obtained auto-ignition time delays in the range similar to those obtained in the current study but at the temperatures 300K higher.

It should be noted however that most of other researcher's data shown on the Figure 22 was obtained in electrically preheated and not in the vitiated air flow. The only vitiated air flow data was obtained by Mullins with fuel spray of big droplets with Sauter Mean Diameter (SMD) of 98μm, which was much larger size than that evaluated for the current study (SMD~30 μm). Spadaccini's data presented on the Figure 22 was in fact obtained in a high pressure reactor with electrically heated air and was transformed to atmospheric conditions by multiplying by pressure squared (e.g., $t_{ign.}=t_{ign.meas@P.}\times P^2$) due to correlations obtained in his experimental series, which in fact represents extrapolation of the experimental data.

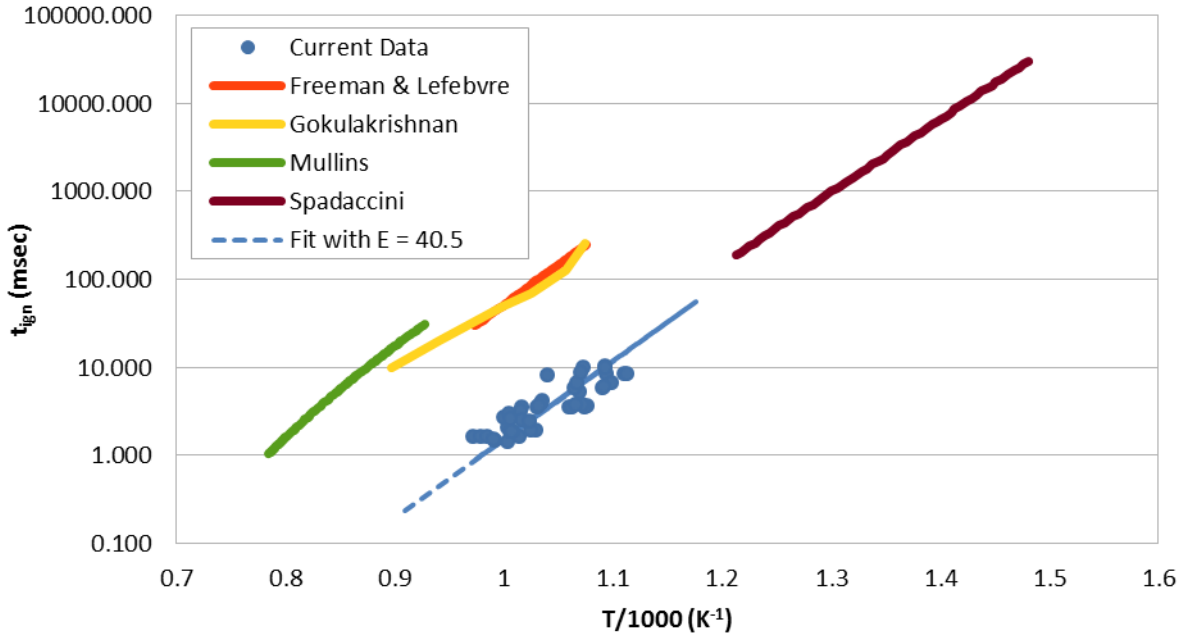

Figure 22. Comparison of auto-ignition delay times obtained in this study to other published results. A curve fit with E_a = 40.5 is superimposed on current data.

It is worth to note that in spite of the different auto-ignition time delays measured by different researches including current study all the lines on the Figure 22 characterizing dependence of the time delay upon temperature have approximately the same slope. This slope corresponds to the power near exponent in the Arrhenius equation [12], which characterize reaction intensity.

$$K = Ae^{-\frac{E_a}{R_u T}} \tag{6}$$

Where K is the reaction rate, A is constant characterizing experimental conditions, E_a is activation energy which is the minimum amount of energy required for a specific reaction to occur, R_u and T are universal gas constant and temperature in degrees Kelvin respectively. As the ignition time delay, $t_{ign,}$ is inversely proportional to K , so

$$t_{ign} \propto e^{\frac{E}{R_u T}}. \quad (7)$$

Thus, the slope of the lines in Figure 22 was determined by the activation energy in the form of

$$Slope = \frac{E_a}{R_u * 1000}. \quad (8)$$

Activation energy reported by different researchers are presented in the Table II and range from E_a*=38 to 45.5 kcal/mole*. The line corresponding to the average activation energy of E_a*=40.5 kcal/mol* was superimposed on the data obtained in the current study. Thus a good agreement between the current and previous studies in terms of activation energy was demonstrated.

Table II. Activation energy reported by different authors

Source	Activation Energy (kcal/mole)	Fuel
Mullins [5]	45.5	Liquid kerosene
Spadaccini&TeVelde [7]	37.8	Liquid Jet-A
Freeman & Lefebvre [8]	40.9	Vaporized kerosene
Gokulakrishnan et al. [9]	38.0	Vaporized JP-8

Conclusions

Auto-ignition delay times were successfully measured using chemiluminescence imaging of the reaction zone. Image sets were recorded at 50 different operating conditions. During these tests velocity of the flow varied in the range of V=80m/sec to 14m/sec. Temperature and percentage of oxygen in the vitiated air flow from T=898K to 1028K and 9.3% to 12.2% respectively. Equivalence ratio of the mixture was varied between φ=0.3 to φ=1.5.
Results show that:

- Ignition delay time increases exponentially with inverse of temperature. Character of the dependence was similar to other researches in terms of activation energy demonstrated by approximately the same slope of the line $t_{ign.}$ *vs. 1000/T* in the log-linear scale. Time delay obtained in the current study was found to be significantly shorter then determined by the other researchers.
- Significant spread of data was observed in the range of lower temperatures (T<950K) due to stronger dependence upon the equivalence ratio and greater unsteadiness of the flame position at lower temperatures.

Future Work

- Future work will expand the range of flow conditions at which auto-ignition delay is determined, with emphasis on higher velocity. Increase of flow velocities will allow characterization of auto-ignition at higher temperatures of the flow.
- Special attention will be given to characterization of the incoming flow conditions and

fuel injection. Boundary layers and test section velocity profile will be measured using Laser Doppler and Particle Image Velocimetry (LDV and PIV respectively). Fuel spray will be characterized using Phase Doppler Particle Analyzer (PDPA).

- In the next experiments, auto-ignition will also be imaged using a high speed camera to study statistics of ignition location to address the observed un-steadiness of auto-ignition delay captured in the time averaged images at the same operating conditions.
- Uniformity of fuel distribution over the cross-section and shape of the flame will be characterized using Planar Laser Induced Fluorescence (PLIF) of jet fuel and OH*.
- Finally, effect of injection of partially oxidized (POX) combustion products upon the auto-ignition process will be characterized in terms of necessary energy addition for flame stabilization at the desired location in a wide range of operating conditions as required in the jet engine afterburner

Acknowledgements

This research was funded by Innovative Scientific Solutions, Inc with contract monitor Larry Goss. The authors would like to thank Anand Agrawal for his support in collecting and processing data, Dmitriy Shcherbik for his assistance in instrumentation of the experimental facility and development of the operational software, and Oleksandr Bibik for his aid in setting up the optical system. This material is based upon work supported by the National Science Foundation Graduate Research Fellowship under Grant No. (DGE-1148903)

REFERENCES

[1] Williams, Alan. Combustion of Liquid Fuel Sprays. London [England]: Butterworths, 1990.

[2] Mullins, B.P., "Studies on the Spontaneous Ignition of Fuels Injected into a Hot Air Stream, Part I-VIII," AGARDograph, No. 4, 1955.

[3] Tacina, Robert. "Autoignition in a Premixing-Prevaporizing Fuel Duct Using Three Different Fuel Injection Systems at Inlet Air Temperatures to 1250K," NASA TM-82938, May 1983.

[4] Spadaccini, L.J., and TeVelde, J.A., "Autoignition Characteristics of Aircraft-Type Fuels," NASA CR-159886, June 1980.

[5] Freeman, G., and Lefebvre, A.H., "Spontaneous Ignition Characteristics of Gaseous Hydrocarbon-Air Mixtures," Combustion and Flame, 58, pp153-162, 1984.

[6] Gokulakrishnan, P., Gaines, G., Klassen, M.S., Roby, R.J., "Autoignition of Aviation Fuels: Experimental and Modeling Study," 43rd AIAA/ASME/ASEE Joint Propulsion Conference, July 2007, Cincinnati, OH, AIAA Paper No.: 2007-5701-138.

[7] Gokulakrishnan, P., Gaines, G., Currano, J., Klassen, M.S., Roby, R.J., "Experimental and Kinetic Modeling of Kerosene-Type Fuels at Gas Turbine Operating Conditions," Journal of Engineering for Gas Turbines and Power, Vol. 139, 2007.

[8] Fuller, C.C., Gokulakrishnan, P., Klassen, M.S., Roby, R.J., and Kiel, B.V., "Investigation of the Effects of Vitiated Conditions on the Autoignition of JP-8," 45th AIAA/ASME/ASEE Joint Propulsion Conference, August 2009, Denver, CO, AIAA Paper No.: 2009-4925.

[9] Birmaher, Shai, "A Method for Aircraft Afterburner Combustion Without Flame Holders," Ph.D. Dissertation, Georgia Institute of Technology, 2009.

[10] Birmaher, S., Zeller, S., Wirfalt, P.W., Neumeier, Y., and Zinn, B.T., "Fuel Injection Scheme for a Compact Afterburner Without Flame Holders," Journal of Engineering for Gas Turbines and Power, V. 130, No. 3, May, 2008.

[11] Cutright, J.T., Neumeier, Y., Zinn, B.T., et al., "Ignition Triggering of Afterburner Fuel Using Partial Oxidation Mixtures," Proc. of ASME Turbo Expo, Orlando, FL, June 2009, GT2009-60157.

[12] Law, Chung K.. Combustion Physics. New York: Cambridge University Press, 2006.

APPENDIX A: Calculated Auto-ignition Delay Times for all Test Conditions

Date	Video #	Temp (K)	Velocity (m/s)	O_2 %	Jet-A Phi	τ_{ign} (ms)
20120606	8	900	103.1	11.8	0.789	8.302
	9	898	102.6	11.9	1.028	8.343
	10	961	106.1	10.9	0.384	8.068
	11	965	105.8	10.9	0.620	4.092
	12	966	105.6	10.9	0.960	3.878
	13	996	103.6	10.2	0.364	2.031
	14	985	103.5	10.2	0.602	1.623
	15	1028	104.3	9.3	0.344	1.611
	16	1021	104.4	9.3	0.551	1.609
	17	1015	104.3	9.3	0.780	1.611
	18	983	141.4	11.9	0.411	3.518
	19	984	141.5	11.9	0.573	3.224
	20	983	141.5	11.9	0.777	2.497
	21	999	140.0	11.6	0.366	2.672
	22	996	140.0	11.6	0.591	1.416
	23	993	140.0	11.6	0.781	
	24	995	140.1	11.6	0.323	3.003
	25	994	140.1	11.6	0.410	2.632
20120611	2	971	88.2	10.7	1.001	1.905
	3	975	88.2	10.7	1.002	1.905
	4	976	87.1	10.8	0.786	2.465
	5	929	86.1	11.6	1.047	3.643
	6	931	86.1	11.6	1.501	3.507
	7	933	85.2	11.7	0.558	3.782
	8	943	86.1	11.6	0.986	3.542
	9	941	86.1	11.6	1.484	3.459
	10	938	86.1	11.6	0.514	3.762
	11	991	91.1	10.9	0.968	1.844
	12	993	90.8	10.9	0.468	1.850
	13	992	90.2	11.0	1.483	1.863
	14	1008	114.7	11.5	1.037	1.465
	15	1009	115.6	11.4	0.462	1.525
20120615	4	915	83.7	12.1	0.482	10.227
	5	914	83.0	12.2	1.003	8.385
	6	910	84.9	11.9	1.519	6.628
	7	915	83.8	11.9	0.546	10.074
	8	917	83.4	11.9	1.059	5.829
	9	916	83.5	11.9	1.486	5.989
	10	932	82.7	11.9	0.461	10.034
	11	933	84.4	11.6	0.950	Flashback
	12	934	83.3	11.8	0.930	Flashback
	13	936	81.2	12.1	0.907	Flashback
	14	936	84.3	11.6	0.944	Flashback
	15	935	81.8	12.0	0.933	Flashback
	16	935	83.8	11.7	0.941	5.185
	17	939	82.5	12.0	1.420	5.818
	18	970	100.4	11.2	0.524	3.512
	19	969	99.9	11.4	0.997	3.673
	20	937	99.3	11.4	1.014	6.621
	21	934	98.6	11.4	1.544	8.547